



Micron-sized ore powder production by propulsion and rapid unloading of high-pressure gas

Fan Yongbo¹ · Qiao Jiyan¹ · Li Shihai¹ · Feng Chun¹

Received: 1 April 2021 / Revised: 24 August 2021 / Accepted: 27 August 2021 / Published online: 6 September 2021
© Australian Ceramic Society 2021

Abstract

We describe a micron-sized ore powder production by propulsion and rapid unloading of high-pressure gas. The research consists of three parts. Firstly, we obtain the tensile strength parameters and permeability coefficient based on the experiment. Secondly, gas propulsion pressure and gas infiltration pressure of the powdering experiment are confirmed. Thirdly, the ore will be fragmented into micron-sized powder when rapid unloading occurs. The grain size analysis indicates that more particles with smaller sizes are obtained at a higher propulsion gas pressure. Particles less than 0.147 mm obtained at the 65 MPa gas propulsion pressure account for 63% of the sample. The critical gas propulsion pressure is determined to be 55 MPa when the volume ratio is 1:3. Powdering experiments show that this method is suitable for metallic and non-metallic ores.

Keywords Gas propulsion pressure · Rapid unloading · Micron-sized powder

Introduction

Steel is an alloy of ore powders and carbon that is vital to the global economy. Its unique combination of strength, formability, and low cost makes it an ideal material for machinery manufacture, construction industry, railway construction, engineering applications, and so on [1]. Ore is the primary raw material from which metallic iron is extracted to make steel.

As summarized in Table 1, Australia has the largest reserves in terms of both crude ore and iron content, followed very closely by Brazil with slightly higher in situ iron grades. Russia is also well placed concerning its ore reserves and in situ grade, but clearly, China is less well endowed. China is endowed with ore reserves of about 23 Bt. However, China's reserves are relatively low grade, averaging about 31% iron, and hence contain only 7.2 Bt [2]. So the contained iron is only about half that for Russia. Currently, China is the largest ore-importing country and has imported about 65% of the world's seaborne ore since 2013, followed

by Japan (11%), Europe (10%), and Korea (6%) as shown in Fig. 1.

Before smelting, the ore must be broken utilizing mechanical methods such as crushing and milling because of lower-grade content. The industrial production of iron powder started in 1937 in the USA [3, 4]. Ore powder production is generally executed by the ball milling method that requires reduplicative ball milling [5]. Multi-stage crushing together with the ball milling process has the characteristics of many processes, high energy consumption, and high cost. There has been extensive research on the ball milling of ore [6–9].

Similarly, the most common way to manufacture Portland cement is through a dry method [10], which involves several stages. The first crushing reduces the limestone to a maximum size of about 6 in. The limestone then goes to secondary crushers or hammer mills for reduction to about 3 in. or smaller [11]. The crushed limestone combined with other ingredients will be heated at about 2700°C. Finally, cement plants grind it by ball milling. Cement grinding is the last step in cement manufacturing and the most energy-intensive process [12].

At present, multi-stage crushing together with the ball milling method focuses on the optimization of steel ball performance; little attention has been paid to the pulverizing mechanism of ore. Compression-shear or tension-shear is the main failure mode during the ball milling process. As we all know, the tensile strength of ore is much lower than

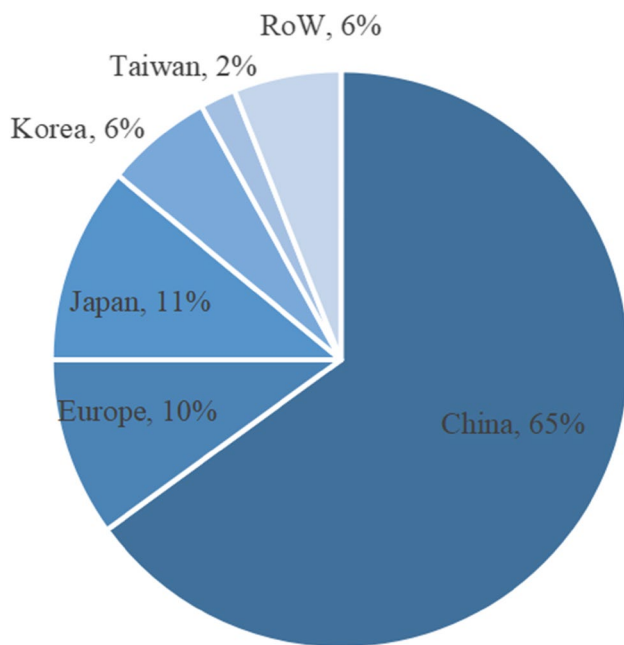
✉ Fan Yongbo
ybfan@imech.ac.cn

¹ Key Laboratory for Mechanics in Fluid Solid Coupling Systems, Institute of Mechanics, Chinese Academy of Sciences, Beijing, China

Table 1 Estimated iron ore reserves in 2013 in the main iron ore-producing countries

Rank	Country	Iron ore reserves (Mt)	
		Unprocessed ore	Iron content
1	Australia	35,000	17,000
2	Brazil	31,000	16,000
3	Russia	25,000	14,000
4	China	23,000	7200
5	India	8100	5200
6	Venezuela	4000	2400
7	Canada	6300	2300
8	Ukraine	6500	2300
9	Sweden	3500	2200
10	The USA	6900	2100
11	Iran	2500	1400
12	Kazakhstan	2500	900
13	South Africa	1000	650
	Other countries	14,000	7100

Source: US Geological Survey (2014)

**Fig. 1** Distribution of world seaborne iron ore trade by destination in 2013 (RoW, rest of the world)

the compressive strength or shear strength. If the ore can be pulverized into powder by an individual overcoming tensile strength, thus much energy could be saved.

Based on overcoming tensile strength separately, micron-sized particle production of ore by rapid unloading of liquid CO₂ was demonstrated [13, 14], which indicates that an explosive may gradually be replaced by a high initial

water pressure until no explosives are used. Unfortunately, this does not appear to be correct now after three experiments with only rapid unloading of high initial water pressure have been conducted. Without any explosives, at initial water pressures of 100 MPa, 165 MPa, and 175 MPa, the proportions of ore particles less than 0.5 mm are only 10%, 30%, and 30%, respectively. As the initial water pressure increases, the proportion of pulverizing no longer changes, which indicates that only a small part of ores can be pulverized into powder. This phenomenon demonstrates that high-pressure gradients generated by water cannot maintain the high pressure inside the ore when there is not any high-pressure gas propulsion. So, high-pressure gas propulsion is the necessary condition for ore pulverization.

A pulverization method for micron-sized ore powder production by high-pressure gas propulsion is proposed. In this paper, we discuss the methods and pulverizing mechanism of ore powder production by high-pressure gas propulsion. We design a series of ore pulverization experiments under different gas pressure propulsion to explore the pulverizing mechanism. Therefore, optimizing the high-pressure gas value by the analysis of particle size distribution of ore powder is the purpose of this article.

Method

Ball milling has three characteristics: (1) “external” loading by mechanical pressure; (2) partial loading; (3) overcome the shear strength or compressive strength. Compared with traditional ball milling, this method has three characteristics: (1) “internal” loading on the ore by applying high pore pressure; (2) through high-pressure gas infiltration, uniform equal stress loading on the ore single crystal scale; (3) overcome the tensile strength by rapid unloading; besides, the whole process of the test only uses water and air, which is a physical separation of the ore and does not change the properties of the ore.

To achieve high-pressure gas propulsion experiments, the high-pressure chamber is divided into two parts: a high-pressure propulsion chamber and a high-pressure infiltration chamber. The volume ratio of the high-pressure propulsion chamber to the high-pressure infiltration chamber is about 1:3. The two parts are connected by an adapter sleeve. Inside of the adapter sleeve, there are a check valve and a thin rupture disk—these objects separate the high-pressure propulsion chamber from the high-pressure infiltration chamber. The two chambers are both full of air added via an inlet control valve1 and valve2. Ore is put into the high-pressure infiltration chamber via the outlet before the thick rupture disk installation. The experimental device is illustrated in Fig. 2. The check valve ensures that the high-pressure gas can discharge successfully while avoiding damage to the thin

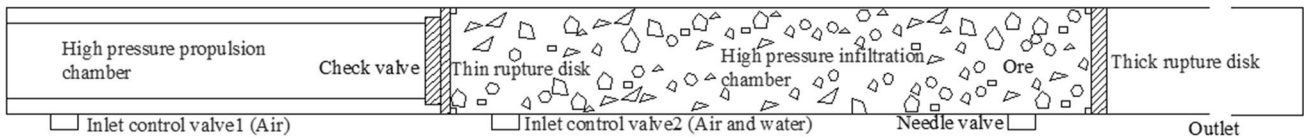


Fig. 2 Schematic diagram of the two high-pressure chambers

rupture disk by the high-pressure air and water from the high-pressure infiltration chamber. After air filling and air substitution, the initial pressure of the air is approximately 40 MPa; the pressure on both sides of the thin rupture disk is raised alternately to maintain the stability of the thin rupture disk.

There are four steps in the whole process. Firstly, ores are put into the high-pressure infiltration chamber. After sealing, the air is injected into the two chambers. Secondly, air substitution in the high-pressure infiltration chamber is executed by high-pressure water. The air inside the ore plays an important role in ore pulverization, and dissociative air can be substituted by water and recycled. Thirdly, high-pressure water initialization can occur very easily after air substitution. Fourthly, the thick rupture disk bursts because of water injection followed by the thin rupture disk bursts. The high-pressure gas pushes the ore to the collection container. The ore will be converted into micron-sized particles because of the high-pressure gradient. A detailed procedure is introduced in the paper [13, 14].

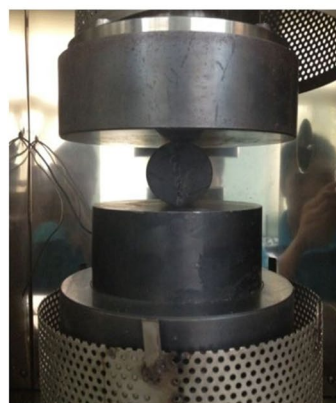
Implementation

Experiment about tensile strength and permeability coefficient

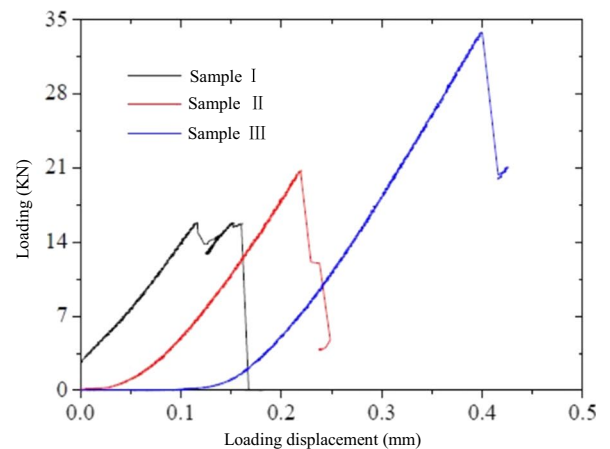
To investigate the basic characteristics of the ore, tension strength and the permeability experiment of the ore are conducted, respectively. The experimental apparatus is a point-loading strength testing machine, as illustrated in Fig. 3. The equation is $\sigma = \frac{2p}{\pi dh}$ (σ , tension strength, Pa; p , failure loading, N; d , diameter of the sample, m; h , thickness of the sample, m). Because of the slight difference of the three samples, three different failure loadings are about 15.75 kN, 20.98 kN, and 33.80 kN. The diameters of the sample I, sample II, and sample III are 50.62 mm, 51.07 mm, and 55.68 mm, and the thicknesses of the sample I, sample II, and sample III are 29.17 mm, 29.86 mm, and 34.96 mm. According to the equation, the tensile strengths are 6.79 MPa, 8.76 MPa, and 11.0 MPa. So the average tension strength of the ore is about 8.85 MPa.

The experimental apparatus is a multifunctional pulse attenuation gas permeability analyzer, as illustrated in Fig. 4. The red line, blue line, and black line in Fig. 4b express upstream pressure, downstream pressure, and confining pressure respectively. According to the equation $(P_u - P_d)/(P_{u0} - P_{d0}) = e^{-\alpha p h a^* t}$ and $\alpha p h a^* = K * A (P_{u0} + P_{d0}) / (2\mu L) * (1/V_u + 1/V_d)$ (P_u , upstream pressure, Pa; P_d ,

Fig. 3 Tensile strength measurement. (a) point loading strength testing machine. (b) loading-displacement curve



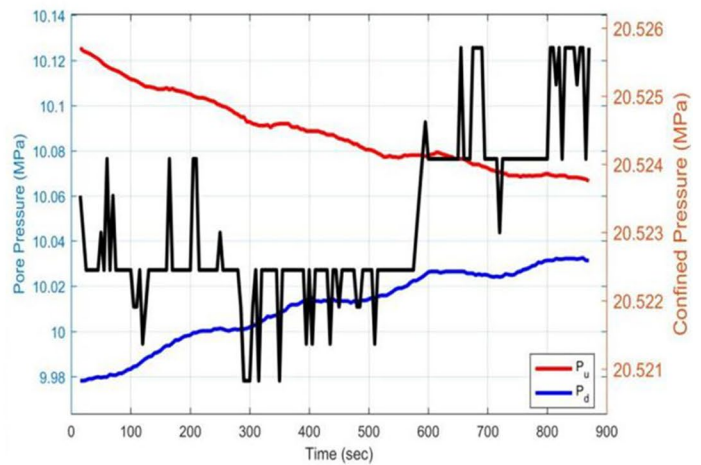
(a) point loading strength testing machine



(b) loading-displacement curve



(a) Multifunctional pulse attenuation gas permeability analyzer



(b) Upstream and downstream pressure versus time curve

Fig. 4 Permeability coefficient measurement. (a) Multifunctional pulse attenuation gas permeability analyzer. (b) Upstream and downstream pressure versus time curve

downstream pressure, Pa; P_{u0} , initial upstream pressure, Pa; P_{d0} , initial downstream pressure, Pa; A , cross-sectional area of the sample, m^2 ; μ , viscosity coefficient of He, Pa*s; L , length of the sample, m; V_u , upstream cavity volume, m^3 ; V_d , downstream cavity volume, m^3), the permeability coefficient of the ore is about 1000nD.

Experiments about ore powdering by propulsion and rapid unloading of high-pressure gas

Based on the conclusions in Section “[Experiment about tensile strength and permeability coefficient](#)” we design four groups of gas propulsion experiments under different values of high-pressure gas. The test apparatus for ore powder production is illustrated in Fig. 5; the volume ratio of the high-pressure propulsion chamber and the high-pressure

infiltration chamber is about 1:3. The schematic diagram of the platform is illustrated in Fig. 6. Ore is the same and fixed close to the thick rupture disk. The propulsion pressure values for the experiments are 45 MPa, 50 MPa, 55 MPa, and 65 MPa, and the infiltration pressure is all 40 MPa. The ore is weighed before being put into the high-pressure infiltration chamber. The equivalent diameter of the ore is < 60 mm because the inner diameter of the high-pressure infiltration chamber is about 63 mm. In each experiment, the quality of the ore is about 1.5 kg, and the equivalent diameter of the ores is between 3 and 5 cm. The volume ratio of ore and water is about 1:1, and the other parameters are presented in Table 2.

The thickness of the thin rupture disk is approximately 1.5 mm, and the diameter of the check valve is approximately 50 mm. The effective shear area of the thin rupture disk is the

Fig. 5 Platform for iron ore powder production

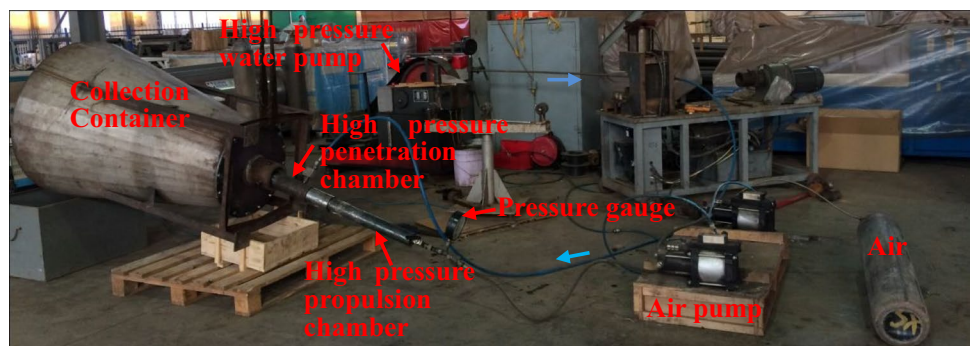
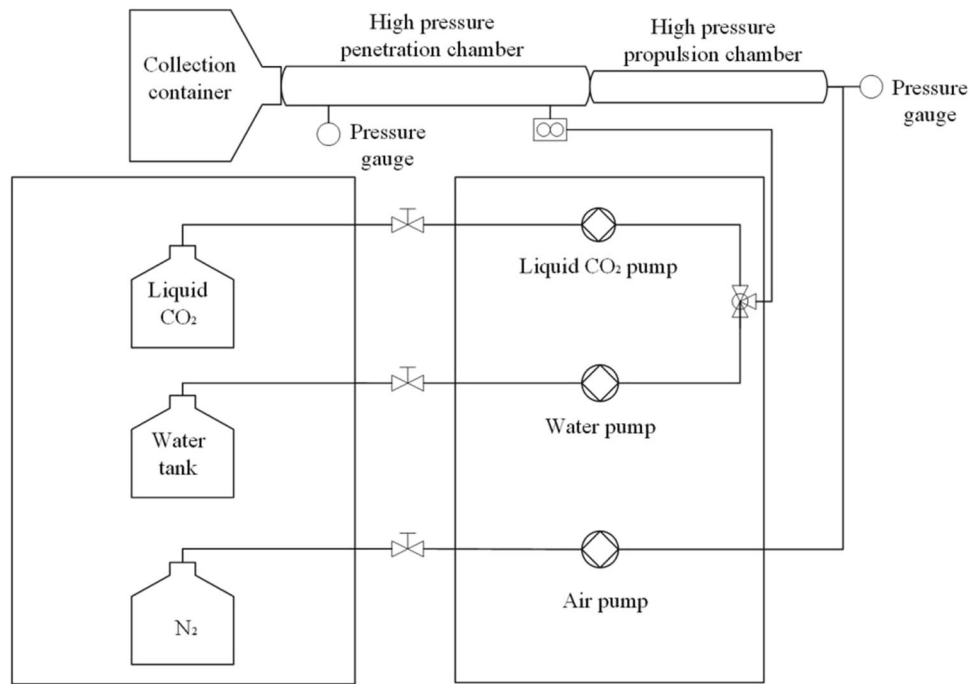


Fig. 6 Schematic diagram of the platform**Table 2** Parameters of powdering under different initial gas pressure

Parameters	The first group	The second group	The third group	The fourth group
The thickness the thin rupture disk (mm)	1.5	1.5	1.5	1.8
The thickness the thick rupture disk (mm)	5.6	5.5	5.6	5.7
Propulsion gas pressure (MPa)	45	50	55	65
Infiltration gas pressure (MPa)	40	40	40	40
The depth and diameter of the check valve (mm)	7,50	7,50	7,50	7,50
The inner diameter and length of the high-pressure gas chamber (mm)	50, 550	50,550	50,550	50,550
The inner diameter and length of the high-pressure liquid chamber (mm)	63, 1000	63,1000	63,1000	63,1000

area of the check valve; thus, the shear strength of the thin rupture disk is approximately 56 MPa. To ensure the stability of the thin rupture disk during the high-pressure gas initialization, the gas pressure above water pressure can not exceed 20 MPa. The pressure on both sides of the thin rupture disk is raised alternately.

After air filling, i.e., air substitution, the equipment is put into the collection chamber. The pressure values on both sides of the thin rupture disk are raised alternately. Moreover, propulsion gas pressure is applied before the water pressure initialization. The thick rupture disk is burst by injecting water into the infiltration chamber after the gas pressure and water pressure are all initialized.

Correlation analysis of high-pressure gas and ore particle size distribution

The average particle size, size distribution, and particle shape are related to the powder characteristics [8, 15–18]. Experiments on ore powder production by different gas propulsion pressure are performed.

The ore particles by microscope are illustrated in Fig. 7. The grain size of the ore particles ranges from 20 to 30 μm . The particle size distribution of the ore powder produced by different gas propulsion pressure is illustrated in Fig. 8. As a whole, with the gas propulsion pressure increasing, the proportion of fine particles gradually increases. d_{10} , d_{50} ,

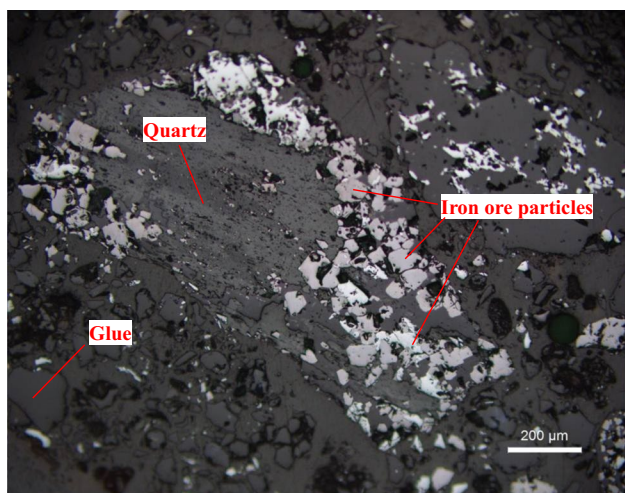


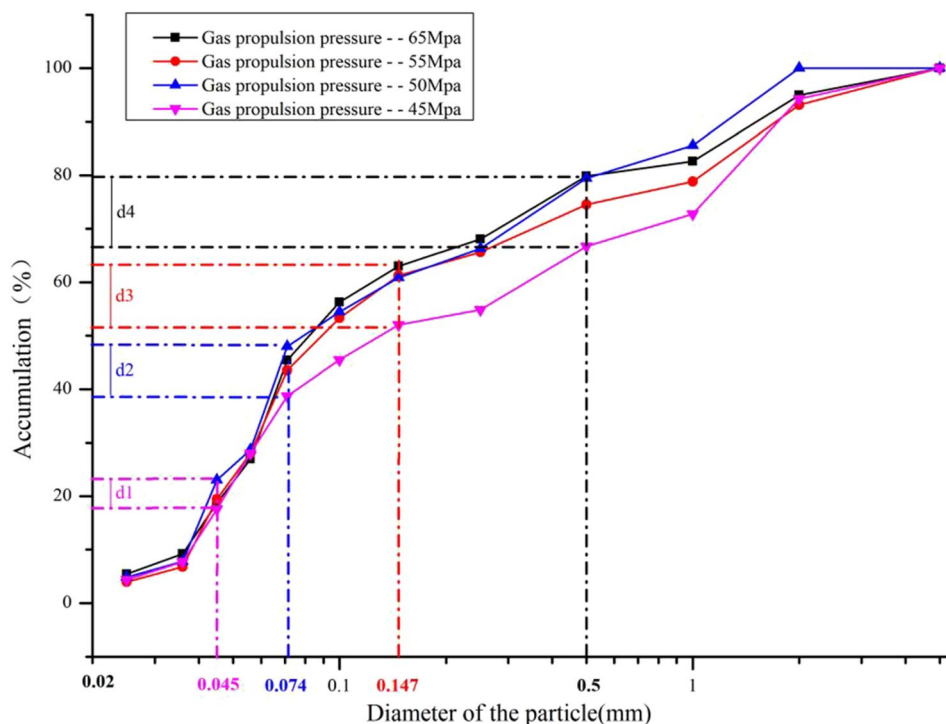
Fig. 7 Iron ore particles by microscope

d3, and d4 represent the difference between the cumulative percentage content (maximum and minimum) of particles less than 0.045 mm, 0.074 mm, 0.147 mm, and 0.5 mm. We could find that d1 is about 5%, which means a variety of gas propulsion pressure has little effect on the total proportion of the particles less than 0.045 mm. That the difference between d4 and d3 is significantly smaller than the difference between d3 and d2 indicates that gas propulsion

pressure increasing contributes to the increase in the proportion of fine particles, and there is an optimal value. Particle sizes less than 0.147 mm account for 52–63% of the particles. We can confirm that the critical pulverizing gas propulsion pressure is determined to be 55 MPa because there is a little difference between the total particles less than 0.147 mm or 0.074 mm when the gas propulsion pressure varies between 55 and 65 MPa. Besides, when the gas propulsion pressure is 55 MPa, the particles between 0.147 and 0.5 mm are lower than the other three groups, and the curve is relatively flat. Correspondingly, when the gas propulsion pressure is 45 MPa, the coarse particles between 1 and 5 mm are significantly higher than the other three groups. The coarse particles between 1 and 5 mm when the gas propulsion pressures are 50 MPa, 55 MPa, and 65 MPa are almost the same.

The role of high-pressure gas propulsion in ore pulverization is vital. High-pressure gas propulsion can ensure the pressure gradient at the moment of ore spouting out of the high-pressure infiltration chamber. The higher the gas propulsion pressure, the faster the ore leaves the outlet. So, a larger proportion of the ore could realize instantaneous unloading, and more small-sized ore powders are obtained. Simultaneously, when the gas propulsion pressure reaches the specific pressure, the powdering result only shows small fluctuations. As a whole, the gas propulsion pressure can be maintained for a relatively long time after the burst of

Fig. 8 Cumulative particle size distribution curve under different gas propulsion pressure. d1, d2, d3, and d4: The difference between the cumulative percentage content (maximum and minimum) of particles less than 0.045 mm, 0.074 mm, 0.147 mm, and 0.5 mm



d1,d2,d3, and d4---The difference between the cumulative percentage content (maximum and minimum) of particles less than 0.045mm, 0.074mm, 0.147mm, and 0.5mm

the thick rupture disk because of the great compressibility of the gas, which ensures the high pressure of the air inside the ore. Under these conditions, the ore can be directly converted into finer powder because the pressure gradient is the greatest. The four cases illustrated above show that this pulverization method is applicable. Particle size distribution can be regulated by controllable methods of the gas propulsion pressure.

To some extent, the initial high-water pressure can maintain and raise the pressure of the air stored in the ore. Thus far, the cooperation of the initial high-water pressure and gas propulsion pressure can ensure the high-pressure gradient inside the ore when the rupture disk bursts instantaneously.

Results and discussion

Generality and reliability of the method

To verify the generality and reliability of the powdering method, many kinds of metallic and non-metallic ore powdering experiments are conducted, such as limestone, bauxite, iron ore, and wood. The results show that the grain size of the particles ranged from 10 to 20 μm , 20 to 30 μm , 20 to 30 μm , and 30 to 40 μm , respectively, as illustrated in Fig. 9. Take iron ore and wood data as examples, as a whole, the particles range from 20 to 40 μm ; they are almost equal. In the range of fewer than 30 μm , the distribution of iron

ore particles is a little higher than that of wood particles, simultaneously. In the range of larger than 35 μm , the distribution of iron ore particles is a bit lower than that of wood particles, which shows that wood is relatively difficult to pulverize than iron ore because of the existence of long fibers. This powdering method is more suitable for brittle materials rather than ductile materials. The particle size distribution as a whole is all normally distributed. The results confirm that this method is suited for metallic and non-metallic ore powder production.

On the industrial scale, first of all, 10-cm ore pulverization has been carried out and proved feasible because there is almost no difference in the results of ore pulverization of different scales, as illustrated in Fig. 10. The volume ratio of the high-pressure propulsion chamber and the high-pressure infiltration chamber is about 14:1, so the gas propulsion pressure and infiltration pressure are both reduced.

Economic and efficiency analysis

Power consumption is a linear function of compressed air usage. The amount of air used to produce ore powder varies based on the scale of the production. If the porosity is about 1%, then it means 99% of the air can be recycled, because only the air penetrating into the pores is necessary to pulverize the ore. We assume that the propulsion gas can be recycled, but ignore the re-compression cost of propulsion gas. Take the infiltration pressure of 40 MPa as an example,

Fig. 9 Four powder particle size distribution curves

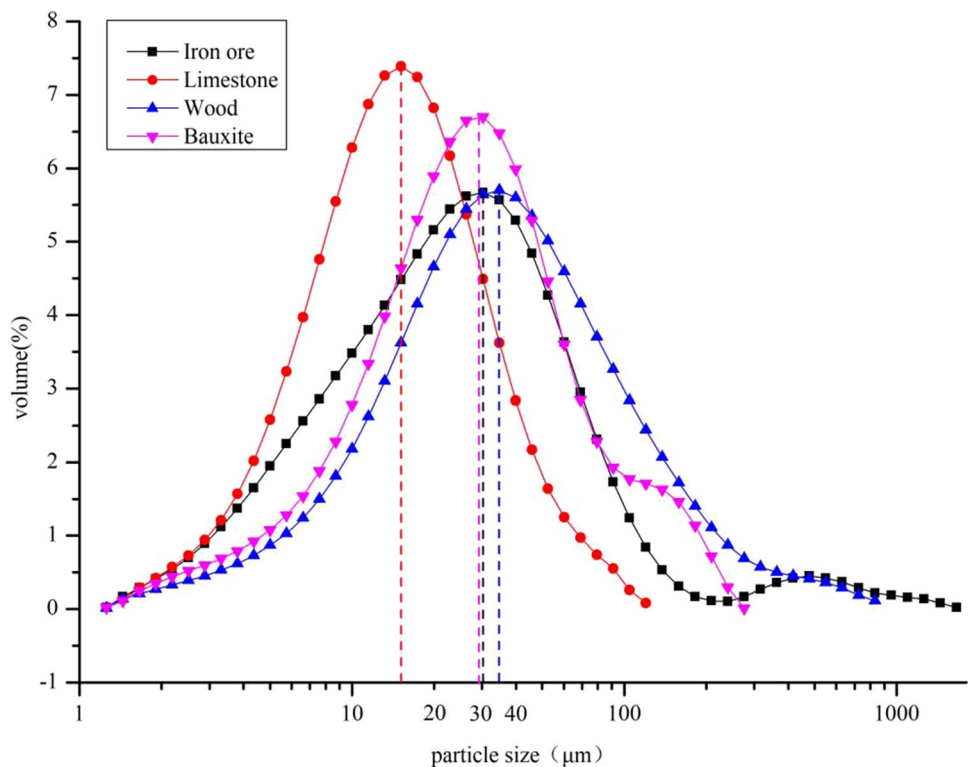
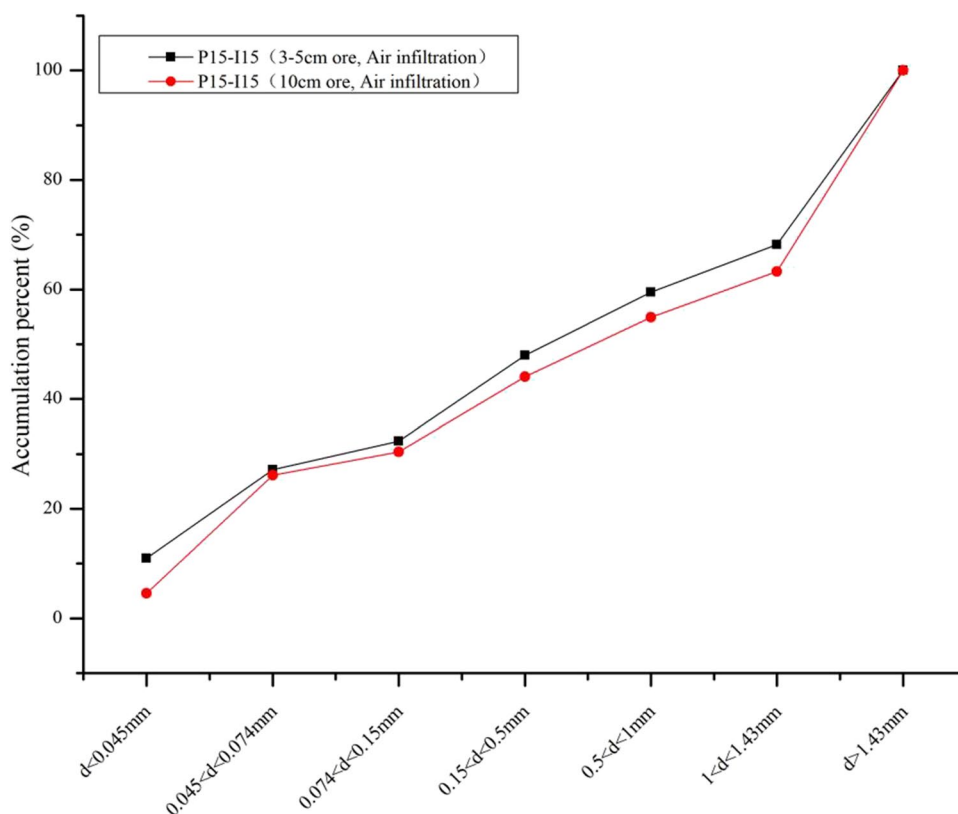


Fig. 10 Cumulative particle size distribution curve about different sizes



completely pulverize 1.5 kg of ore into ore powder less than 0.074 mm, and the power consumption is about 0.83 kWh. The power price in China is 0.054 \$ per kWh for industry usage. So the power consumption for one ton of ore is about $0.83 * 0.054 * 1000 / 1.5 = 28.8$ \$ because the air consumption is only 1%, so the power consumption is estimated as $28.8 * 0.01 = 0.288$ \$ per ton of iron ore.

Discussion about technology and scheme optimization

Based on the comparison of pulverizing experiments at different gas propulsion pressure, there is now a consensus that there is an optimal gas pressure when the volume ratio is about 1:3. Further studies are needed to optimize gas propulsion pressure initialization. The pulverizing effect is positively related to the total propulsion energy, so it can be considered to increase the gas volume and reduce the gas pressure. When the volume ratio is within a reasonable range, we can reduce the manufacturing cost of the high-pressure container.

Also, we consider keeping the gas propulsion pressure constant and changing the infiltration pressure in subsequent experiments. A comprehensive analysis will be discussed about the infiltration pressure and gas propulsion pressure on the particle size distribution, to optimal pressure combination design.

Why are there always coarse particles? In other words, the particle size distribution curve shows a normal distribution as a whole. What improvements can achieve uniform distribution are issues that we need to consider.

Conclusions

A pulverization method for micron-sized ore powder production by propulsion and rapid unloading of high-pressure air is introduced. This approach is different from the traditional ball milling process based on the compression-shear or tension-shear. The experiments approve that the pulverization method is applicable.

More small particles are obtained at a higher gas propulsion pressure. When the volume ratio is 1:3, particles less than 0.147 mm obtained from the 65 MPa pressure gas accounted for 63%, and there are very few differences about the total particles less than 0.147 mm or 0.074 mm when the gas propulsion pressure varies between 55 and 65 MPa. Thus, 55 MPa gas propulsion pressure when the volume ratio is 1:3 is considered to be critical pulverizing conditions. Simultaneously, this method is suited for metallic and non-metallic ore powder production.

Acknowledgements The authors would like to sincerely thank Guo WX and Liu HQ for their help with the laboratory equipment. We are

grateful for the support by the National Key Research and Development Project (2018YFC1505504) and the National Natural Science Foundation of China (11802313).

Funding The work presented in this paper was supported by the National Key Research and Development Project (2018YFC1505504) and the National Natural Science Foundation of China (11802313).

Declarations

Conflict of interest The authors declares no competing interests.

References

1. Wu, S.P., Meng, S.Y.: Preparation of micron size copper powder with chemical reduction method [J]. *Mater. Lett.* **60**, 2438–2442 (2006)
2. Jacques, F., Hubert, L., Jean, J.L., et al.: Particle generation for pharmaceutical applications using supercritical fluid technology [J]. *Powder Technol.* **141**, 219–226 (2004)
3. Thummler, F., Oberacker, R.: *Introduction to Powder Metallurgy*, Oxford Science Publications, 1993, 346
4. German, R.M.: *Powder Metallurgy of Iron and Steel*, JohnWiley & Sons, Inc, 605 Third Ave, New York, NY 10016, USA, 1998, 496
5. Wolff, A.P., Costa, G.M., Dutra, F.C.: A comparative study of ultra-fine ore tailings from Brazil. *Mineral processing and extractive. Metall. Rev.* **32**(1), 47–59. <https://doi.org/10.1080/08827508.2010.530718>
6. Peng, Y.X., Ni, X., Zhu, Z.C., et al.: Friction and wear of liner and grinding ball in ore ball mill [J]. *Tribol. Int.* **115**, 506–517 (2017)
7. Sakthivel, R., Jayasankar, K., Das, S.K., et al.: Effect of planetary ball milling on phase transformation of a silica-rich ore [J]. *Powder Technol.* **208**(3), 47–751 (2011)
8. Ghambari, M., Shaibani, M.E., Eshraghi, N.: Production of grey cast iron powder via target jet milling. *Powder Technol.* **221**, 318–324 (2012)
9. Casagrande, C., Alvarenga, T. & Pessanha, S.: Study of ore Mixtures Behavior in the Grinding Pelletizing Process, *Mineral Processing and Extractive Metallurgy Review*, <https://doi.org/10.1080/08827508.2016.1244058>
10. Ernst, W., Nathan, M., Lynn, P.: Potentials for energy efficiency improvement in the US cement industry. *Energy* **25**, 1189–1214 (2000)
11. Madloul, N.A., Saidur, R., Rahim, N.A., et al.: An overview of energy savings measures for cement industries. *Renew. Sustain. Energy Rev.* **19**, 18–29 (2013)
12. Sogut, M.Z.: A research on exergy consumption and potential of total CO₂ emission in the Turkish cement sector. *Energy Convers. Manage.* **56**, 37–45 (2012)
13. Fan, Y.B., Duan, W.J., Li, S.H., Qiao, J.Y.: Experiment on micron-sized particle production of iron ore by rapid unloading of liquid CO₂. *Powder Technol.* **327**, 449–455 (2018)
14. Fan, Y.B., Qiao, J.Y., Li, S.H., Feng, C.: Micron-sized silicon carbide particle production by rapid unloading of liquid CO₂. *J. Aust. Ceram. Soc.* **55**, 595–600 (2018)
15. Masoud, B., Sima, R.: Production of micro- and nano-composite particles by supercritical carbon dioxide [J]. *J. Supercrit. Fluids* **40**, 263–283 (2007)
16. Thommes, M., Kleinebudde, P.: The Behavior of Different Carageenans in Pelletization. *Pharm. Dev. Technol.* **13**, 27–35 (2008)
17. Verheyen, P., Steffens, K.J., Kleinebudde, P.: Use of crospovidone as pelletization aid as alternative to microcrystalline cellulose: effects on pellet properties. *Drug Dev. Ind. Pharm.* **35**(11), 1325–1332 (2009)
18. Fu, X., Huck, D., Makein, L., et al.: Effect of particle shape and size on flow properties of lactose powders. *Particuology* **10**(2), 203–208 (2012)

Publisher's note Springer Nature remains neutral with regard to jurisdictional claims in published maps and institutional affiliations.